IMPACT OF RARE EARTH OXIDES ON THE STRUCTURE AND ELECTRICAL PROPERTIES OF ZnO-Bi_2O_3−BASED VARISTOR CERAMICS: A COMPARATIVE ANALYSIS OF Y_2O_3 AND CeO_2

Nguyen Trung Huy, Nguyen Van Trang, Cao Thi Hong, Nguyen Thi Xuyen, Vo Thi Kieu Anh, Nguyen Quang Duong, Nguyen Tuan Anh, Le Dang Quang, Do Quang Tham*

Institute for Tropical Technology, Vietnam Academy of Science and Technology, Ha Noi, Vietnam

ARTICLE INFORMATION

Journal: *Vinh University Journal of Science Natural Sciences, Engineering and Technology*
p-ISSN*: 3030-4563*
e-ISSN: *3030-4180*

Volume: 53
Issue: 2A
****Correspondence:***
dqtham@itt.vast.vn

Received: *27 February 2024*
Accepted: *08 April 2024*
Published: *20 June 2024*

Citation:
Nguyen Trung Huy et al. (2024). Impact of rare earth oxides on the structure and electrical properties of ZnO-Bi_2O_3−based varistor ceramics: a comparative analysis of Y_2O_3 and CeO_2. ***Vinh Uni. J. Sci.*** *Vol. 53 (2A), pp. 89-102*
doi: 10.56824/vujs.2024a022a

ABSTRACT

Zinc oxide (ZnO)-based varistor ceramics, incorporating varying amounts of Y_2O_3/CeO_2, were fabricated through a two-step solid-state reaction method involving pre-calcination and subsequent sintering processes. ZnO powder and corresponding additives served as raw materials in the production. The investigation of phase composition, microstructure, and electrical properties employed techniques such as X-ray diffractometry (XRD), scanning electron microscopy (SEM), and direct current electrical measurement. The findings revealed that varistor ceramics sintered at 950°C, using powder pre-calcined at 800°C and doped with an appropriate amount of Y_2O_3, exhibited enhanced electrical properties. Conversely, the introduction of varying concentrations of CeO_2 did not contribute to the improvement of the electrical characteristics. The CeO_2-doped samples displayed lower breakdown voltages and nonlinear coefficients compared to the undoped sample (M0). The addition of Y_2O_3 proved effective in improving the nonlinear coefficient but resulted in a decrease in the breakdown voltage withstand capability of the samples. A Y_2O_3 content of 0.5% was identified as a suitable compromise, balancing both factors. Notably, ZnO varistors doped with 0.5 mol% Y_2O_3 demonstrated optimal comprehensive electrical properties, featuring a breakdown field of 620 V/mm and a nonlinear coefficient of 45. These results suggest that Y_2O_3 doping holds promise as a viable strategy for achieving varistor ceramics with outstanding electrical performance.

Keywords: Electrical properties; rare earth oxides; ZnO-Bi_2O_3-based varistor; CeO_2, Y_2O_3.

1. Introduction

Zinc oxide (ZnO)-based varistors are extensively employed for overvoltage protection and voltage stabilization due to their capacity to manage significant surges and exhibit nonlinear characteristics. Typically, ZnO-based varistor ceramics are formulated by sintering

ZnO powder with minor additives. In particular, Bi_2O_3 is employed as the varistor-forming agent, introducing nonlinear characteristics to ZnO varistor ceramics. Traditional dopants include various metal oxides such as Sb_2O_3, Co_3O_4, MnO_2, and Cr_2O_3 [1-6]. Throughout the sintering process, these oxides undergo reactions with ZnO, leading to the formation of distinct phases, including the spinel phase $Zn_7Sb_2O_2$, the pyrochlore phase $Zn_2Bi_3Sb_3O_{14}$, and the Bi_2O_3-rich liquid phase. The pyrochlore phase emerges within the temperature range of 750-850°C, and with increasing temperature, it decomposes into spinel and the Bi_2O_3-rich liquid phase at 950-1050°C. Recent investigations have indicated that the incorporation of rare earth elements as dopants can influence the microstructure evolution of ZnO varistors, effectively controlling the grain size of ZnO. For instance, Tu et al. [7] observed that the addition of Y_2O_3 resulted in the formation of a new phase, leading to a reduction in grain size. Additionally, Bernik's group achieved a reduction in ZnO grain size from 11.3 μm to 5.4 μm and an increase in the breakdown field from 150 V/mm to 274 V/mm by adopting a high-temperature solid-phase method and introducing Y_2O_3 to the ZnO-Bi_2O_3 system [8]. This confirmed the efficacy of Y_2O_3 as a potent inhibitor of grain growth, thereby enhancing the breakdown field. K.V. Mahesh et al. incorporated Y_2O_3 into nanosized ZnO powder, resulting in a varistor with a grain size of 2 μm [9]. To summarize, the doping of Y_2O_3 has proven to be an effective and convenient method for improving the electrical properties of ZnO varistors. However, limited research has been conducted on the addition of CeO_2, a widely recognized rare earth oxide (REO), to ZnO-Bi_2O_3 based varistors in the existing literature. Cao et al. reported that the inclusion of CeO_2 led to a decrease in the average grain size from 7.3 to 6.7 μm and an increase in breakdown voltage from 438 to 501 V/mm when the CeO_2 content ranged from 0 to 0.2 mol%. The nonlinear coefficient exhibited an initial increase from 38 to 51 with the addition of CeO_2 up to 0.1 mol%, but further doping resulted in a decrease to 44 at 0.2 mol%. Given the prevailing trend among researchers and manufacturers to focus on achieving varistors with high voltage gradients and improved electrical responses, it is imperative to prioritize investigations into the addition of REOs, such as CeO_2, to the ZnO-Bi_2O_3 based varistor formulation, followed by thorough evaluations.

This study presents the preparation of ZnO-based varistor ceramics through the sintering of pressed disks comprised of pre-calcined powder mixtures of ZnO and various additives. The comparison of the effects of Y_2O_3 and CeO_2 on ZnO-Bi_2O_3 based varistors is undertaken with the aim of achieving an enhanced electrical response for potential applications. Simultaneously, the influence of sintering temperature on the microstructure and electrical properties of the ceramics is systematically investigated.

2. Experimental procedures

Zinc oxide (ZnO)-based varistors were synthesized utilizing the solid-state reaction route. High-purity raw materials with a nominal composition of (95.4-x) mol% ZnO, 0.7 mol% Bi_2O_3, 0.5 mol% Cr_2O_3, 0.5 mol% Co_3O_4, 1.0 mol% Sb_2O_3, 1.0% SiO_2, 0.9 mol% MnO_2, and x% Y_2O_3/CeO_2 (with x values of 0, 0.25, and 0.75 for Y_2O_3, and 0, 0.25, 0.75, and 1% for CeO_2) were meticulously blended through ball milling for 9 hours. The resulting mixture was subsequently dried at 60°C for 12 hours, followed by pre-calcination at 800°C for 1 hour in an air environment. Following pre-calcination, a polyvinyl alcohol solution (5 wt%) was introduced to the pre-calcined powder, and the composite was then pressed into disks (15 mm in diameter and approximately 1.5 mm in thickness) under a pressure of 100 MPa. Subsequently, the disks underwent sintering at temperatures of 900°C, 950°C, 1000°C, or 1100°C for a duration of 2 hours in air. Finally, both surfaces of the sintered disks were meticulously polished and coated with silver paste to create electrodes, which were formed through heat treatment at 400°C for 1 hour. This detailed synthesis process ensures the controlled fabrication of ZnO-based varistors with varying compositions, particularly incorporating Y_2O_3 and CeO_2, for subsequent evaluation of their electrical properties.

The nominal varistor voltages, V_{1mA} and V_{10mA}, were measured at 1 mA and 10 mA by an MY-3 kV meter at room temperature, respectively. The breakdown field, E_b (V/mm), was calculated by the equation:

$$E_b = V_{1mA}/H \quad (1)$$

in which H is the thickness of the specimen in mm.

The nonlinear coefficient α was calculated via the equation:

$$\alpha = 1/\log(V_{10mA} / V_{1mA}) \quad (2)$$

The crystal structure of the samples was characterized using a DX-1000 diffractometer with Cu Kα radiation operating at 40 kV/25 mA. The micrograph of the varistors was characterized via an SEM (J6510-LV) and the elemental distribution of the varistors was characterized by the energy-dispersive X-ray spectroscopy (EDS).

3. Result and discussion

3.1. Effect of REO contents

Figure 1 illustrated the XRD patterns of samples doped with 0.5% of Y_2O_3/CeO_2, in which the ZnO phase, spinel phase ($Zn_7Sb_2O_{12}$), pyrochlore phase ($Zn_2Bi_3Sb_3O_{14}$), Y-rich phase and Ce-rich phase can be determined. After the doping of Y_2O_3/CeO_2, new peaks corresponding to Y-rich phase and Ce-rich phase appear at near 30 deg.

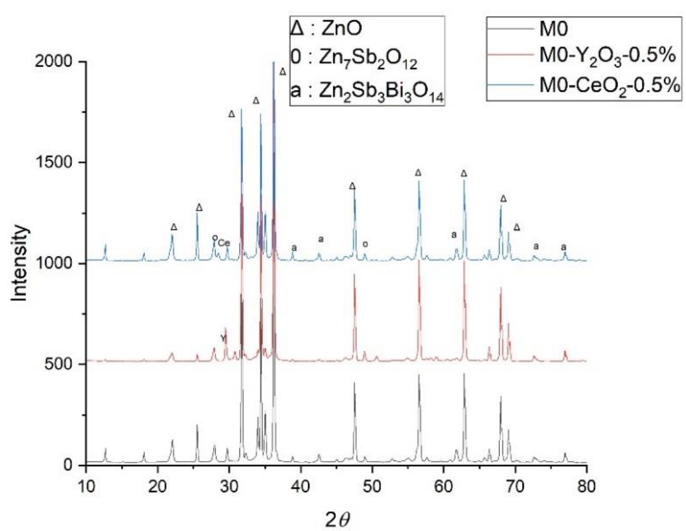

Figure 1: *XRD patterns of ZnO varistors doped 0.5% of Y_2O_3/CeO_2*

The SEM micrographs depicted in Fig. 2 illustrate samples with varying contents of [mention the specific material, e.g., Y_2O_3 or CeO_2]. The results reveal a substantial presence of numerous small particles distributed at the ZnO grain boundaries. As the concentration of rare earth oxides (Y_2O_3 and CeO_2) increases, the quantity of secondary phase particles at the ZnO grain boundaries exhibits a discernible upward trend, resulting in a reduction in the average size of the ZnO particles. This phenomenon can be ascribed to the following factors: the ionic radii of Y^{3+} ions (0.093 nm) and Ce^{4+} ions (0.097 nm) surpass that of Zn^{2+} ions (0.074 nm) [10-12]. Consequently, the solid solubility of Y^{3+} and Ce^{4+} ions in the ZnO grain is notably low. The outcomes of XRD and EDS analyses, as depicted in Fig. 3, further corroborate that Ce^{4+} and Y^{3+} ions predominantly localize at the ZnO grain boundaries, forming Y-rich and Ce-rich phases. These secondary phases effectively impede the growth of ZnO grains through a pinning effect. The intricate interplay between the foreign ions and the ZnO matrix leads to the observed reduction in ZnO particle size, emphasizing the role of rare earth oxides in influencing the microstructural evolution of the varistor material.

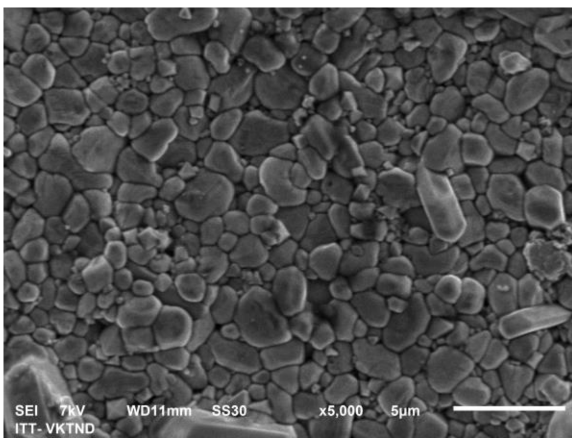

a) M0-950-5k

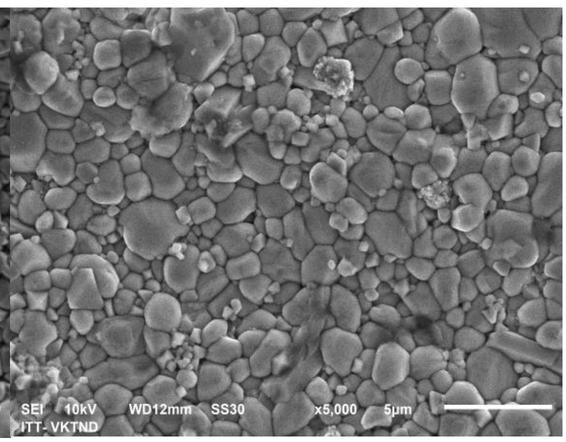

b1) M0-Y_2O_3-0.25-950

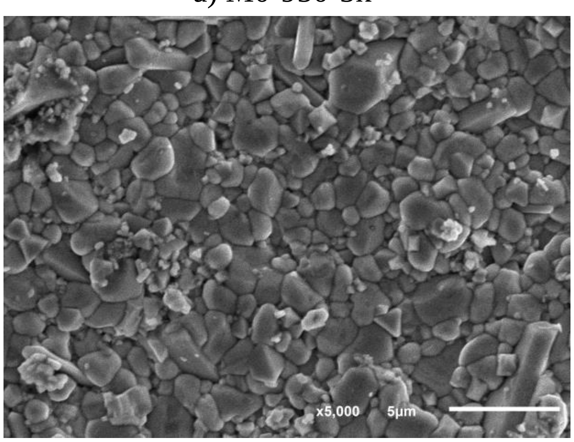

b2) M0-Y_2O_3-0.5-950

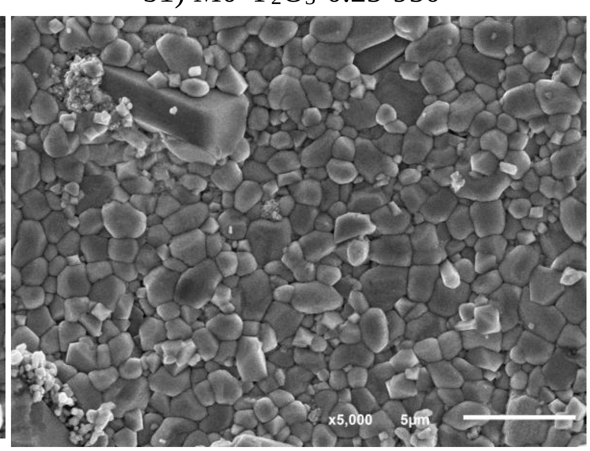

b3) M0-Y_2O_3-0.75-950

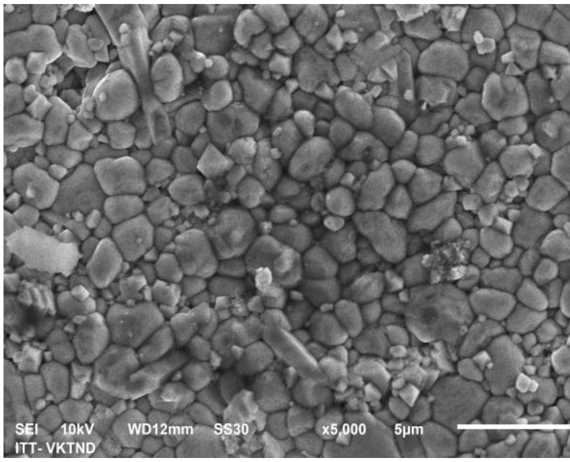

c1) M0-CeO_2-0.25-950

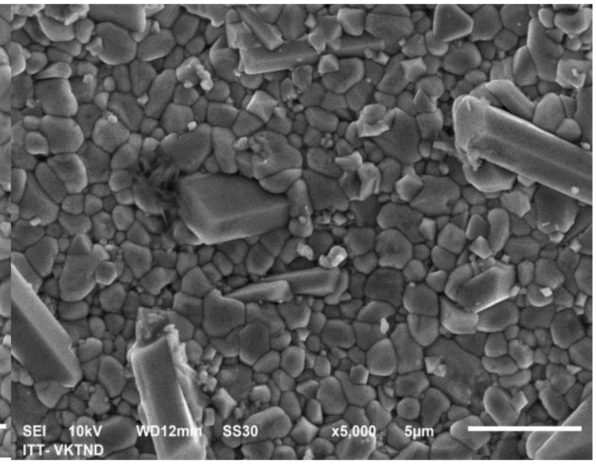

c2) M0-CeO_2-0.5-950

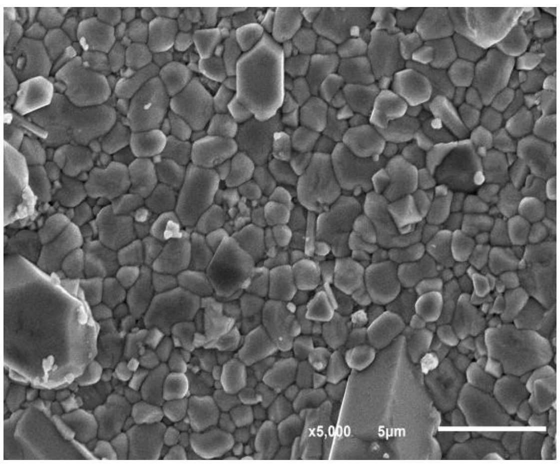

c3) M0-CeO_2-0.75-950

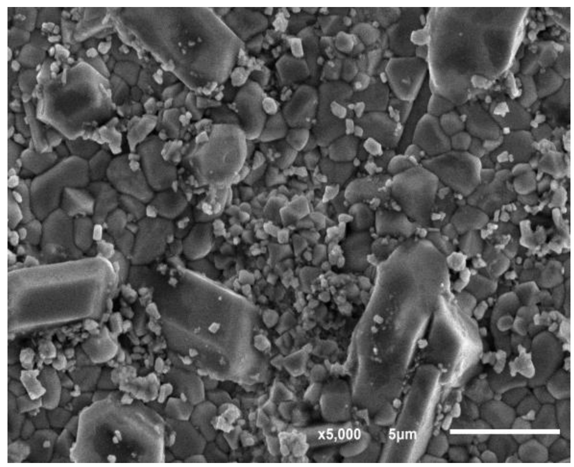

c4) M0-CeO_2-1-950

Figure 2: *SEM micrographs of the samples with different content of Y_2O_3/CeO2: a) x = 0%; b1-b3: x= 0.25; 0.5; 0.75% Y_2O_3; c1-c4: x= 0.25; 0.5; 0.75; 1% CeO_2*

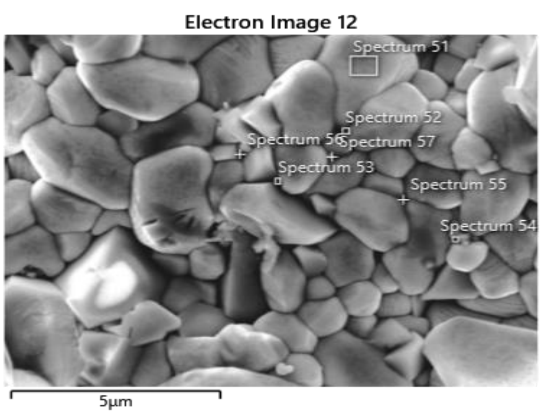

Spectrum	51	54	56
Zn	75.6	45.6	30.8
O	24.2	27.6	13.9
Cr		11.1	5.8
Mn		7.3	7.6
Co		3.1	4.5
Sb		2.8	30.3
Bi		2.3	6.9
Si	0.2	0.2	0.3

a) M0

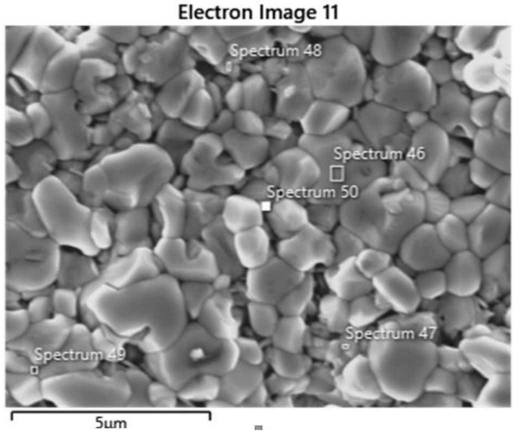

Spectrum	**46**	**47**	**50**
Zn	78.8	68.2	53.8
O	21.2	27.4	26
Sb		1.3	6.3
Bi		1.3	6.6
Si			
Y		1.8	7.3

b) M0-Y_2O_3-0.5-950

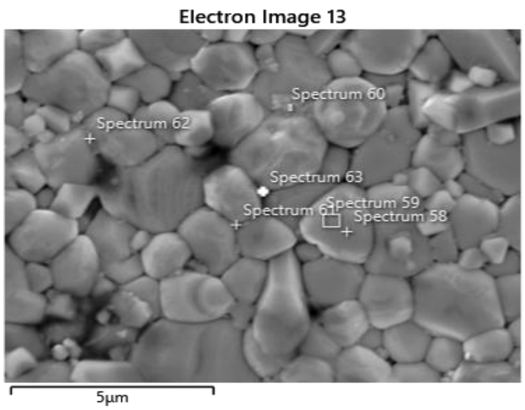

Spectrum	**58**	**60**	**61**
Zn	78.4	28.2	78.5
O	21.6	18.2	19.5
Sb		10	
Bi		14.0	
Si		0.2	
Ce		20.2	2.0

c) M0-CeO_2-0.5-950

Figure 3: *EDS analysis of the sample with/without 0.5% mol of Y_2O_3/CeO_2*

The substitution reaction of Y^{3+}/Ce^{4+} for Zn^{2+} causes lattice defects in ZnO grains, releasing the oxygen during the process, which is represented by the Kroger-Vink [13-15] defect symbol as:

$$Y_2O_3 \xrightarrow{ZnO} 2Y^{\bullet}_{Zn} + 2O^{\times}_{O} + 2e' + 1/2O_2 \quad (3)$$

$$CeO_2 \xrightarrow{ZnO} Ce^{\cdot}_{Zn} + e' + 1/2\ O_2 \quad (4)$$

The defect reaction not only provides O_2 for the enhancement of the interface state density N_s, but also produces positron centers and additional current carriers and the lattice defects and deep bulk traps are formed.

Figure 4 and Table 1 presented below provide a comprehensive overview of the current-voltage (I-V) characteristics and key electrical parameters of the varistor samples, based on experimental data and quality assessments. The research findings indicate a significant influence of the rare earth oxide additives on the threshold voltage values (Eb, V/mm), as well as the nonlinear coefficient α. Notably, the presence of rare earth oxides notably impacted the Eb values. For sample M0, which lacks rare earth oxide additives, the Eb value is 1425 V/mm. However, for samples with rare earth oxide additives, this value significantly decreases. In the case of Y_2O_3-doped samples, the Eb value decreases from 1166 V/mm for the 0.25% Y_2O_3 sample to 1125 V/mm for the 0.75% Y_2O_3 sample. Regarding CeO_2-doped samples, the Eb value exhibits negligible variation at 0.25% and 0.5% doping levels by mass (1400-1420 V/mm). Nevertheless, as the doping level increases to 0.75% and 1% by mass, this value decreases sharply to approximately 1100 V/mm. The analysis of the nonlinear coefficient reveals a contrasting trend between Y_2O_3 and CeO_2 additives. Sample M0 possesses a nonlinear coefficient value of 32, while Y_2O_3-doped samples exhibit values ranging from 30 to 35, and 18-23 for CeO_2-doped samples. These results indicate a significant reduction in the nonlinear coefficient due to CeO_2 doping. The nonlinear coefficient values for Y_2O_3-doped samples may vary depending on the Y_2O_3 content, with the highest coefficient (35) observed for the 0.5% Y_2O_3-doped samples. For CeO_2-doped samples, the 0.5% doping level demonstrates the best electrical characteristics among various doping levels (Eb = 1420; α = 20). At the 0.75% CeO_2 doping level, the nonlinear coefficient is improved (reaching a value of 22); however, the Eb value experiences a notable decrease (down to 1134 V/mm). Therefore, the 0.5% doping level was selected for investigating the influence of sintering temperature.

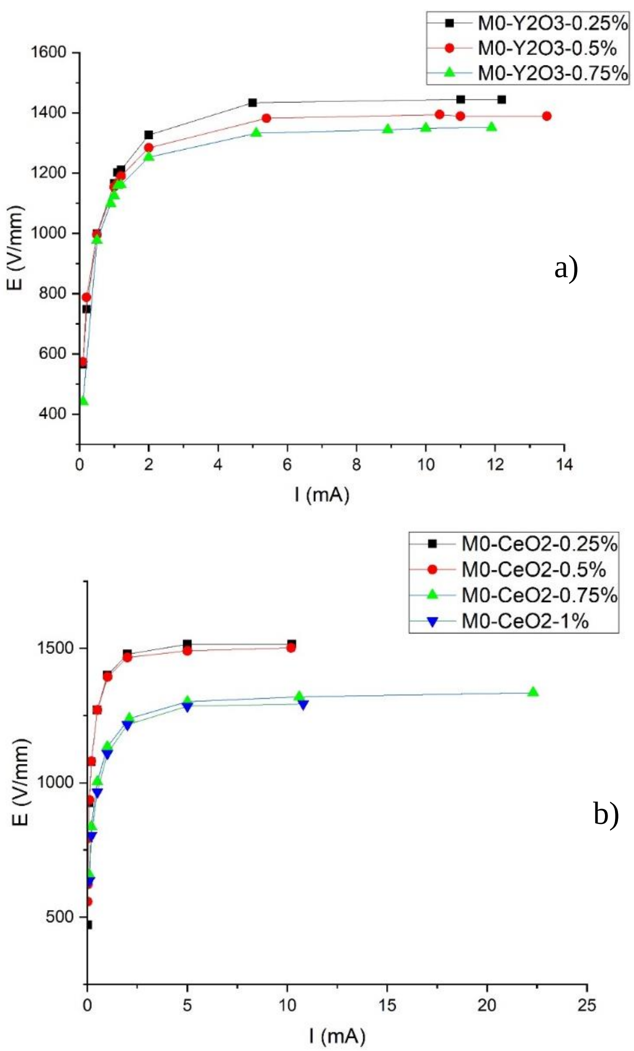

Figure 4: *E-J curves of samples doped with various amounts of Y_2O_3(a) and CeO_2 (b)*

Table 1: *E-J parameters of samples with different content of Y_2O_3/CeO_2*

Samples	E_b (V/mm)	α	Samples	E_b (V/mm)	α
M0	1425	32	M0-CeO_2-0.25%	1400	18
M0-Y_2O_3-0.25%	1166	31	M0-CeO_2-0.5%	1420	20
M0-Y_2O_3-0.5%	1154	35	M0-CeO_2-0.75%	1134	22
M0-Y_2O_3-0.75%	1125	30	M0-CeO_2-1%	1109	23

3.2. Effect of sintered temperature

The specimens underwent sintering at varying temperatures (900-950-1000-1100°C) for a duration of 2 hours, and their SEM images are illustrated in Figure 5 below. The outcomes reveal substantial alterations in the structural characteristics of the specimens with increasing sintering temperatures. The particle sizes of the samples experienced a notable escalation, accompanied by a more tightly organized structure. At 900°C, the structure exhibited significant non-uniformity due to excessively low sintering temperatures, resulting in numerous phases that had not completed the transformation process into the final product. Additionally, an observed trend indicates that as the sintering temperature rises, the ZnO particle sizes also increase significantly, potentially contributing to a reduction in the threshold voltage.

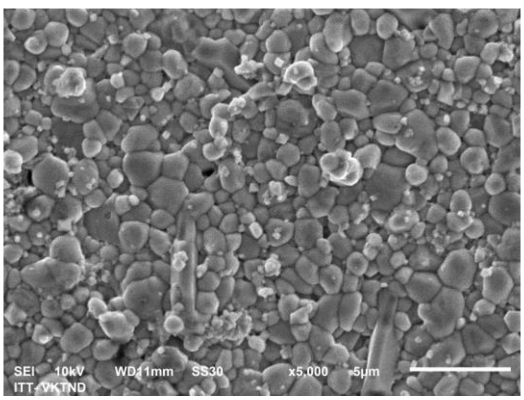

M0-900

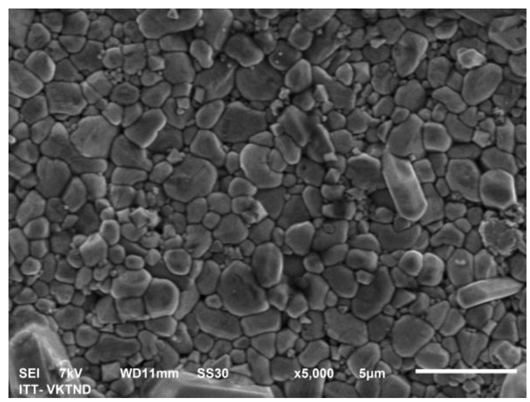

M0-950

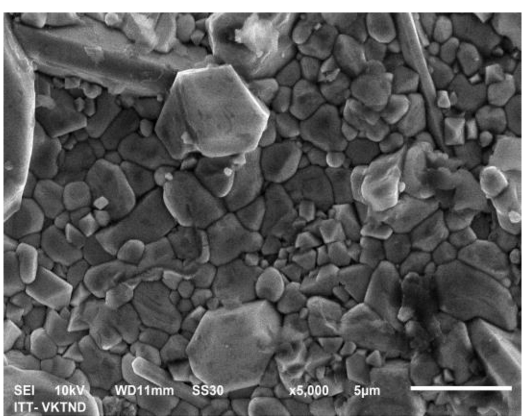

M0-1000

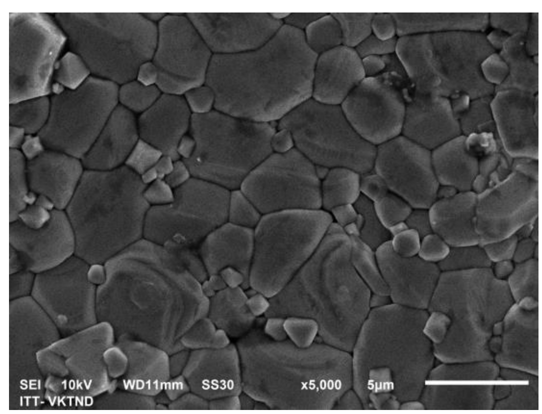

M0-1100

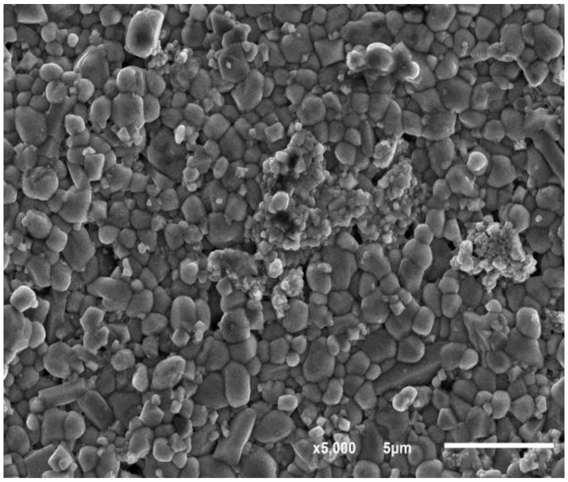

M0-Y_2O_3-0.5-900

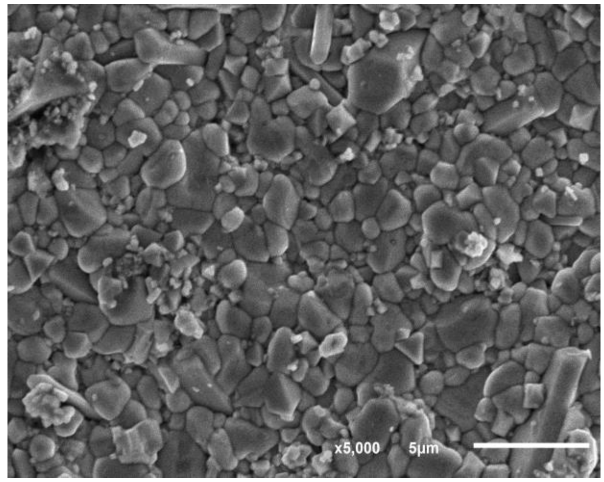

M0-Y_2O_3-0.5-950

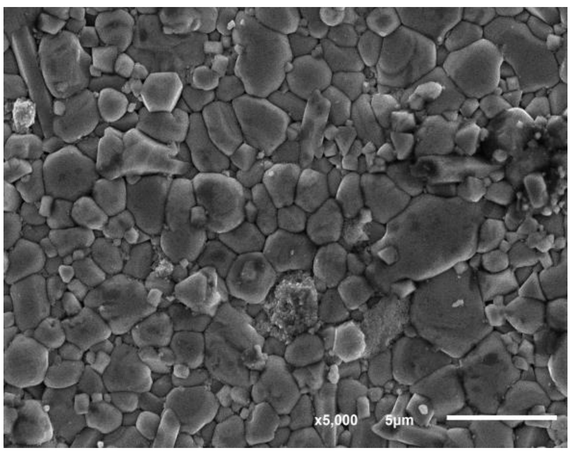

M0-Y_2O_3-0.5-1000

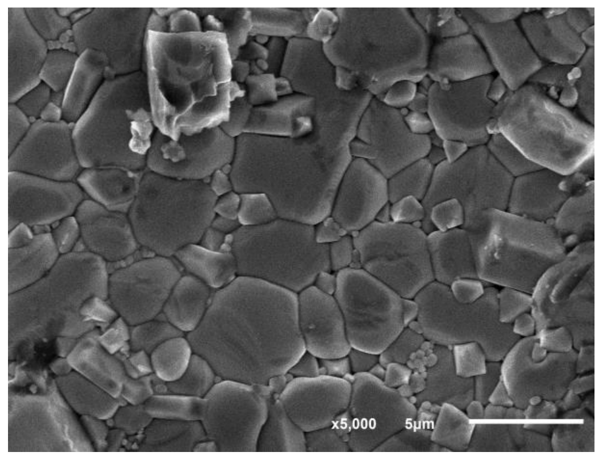

M0-Y_2O_3-0.5-1000

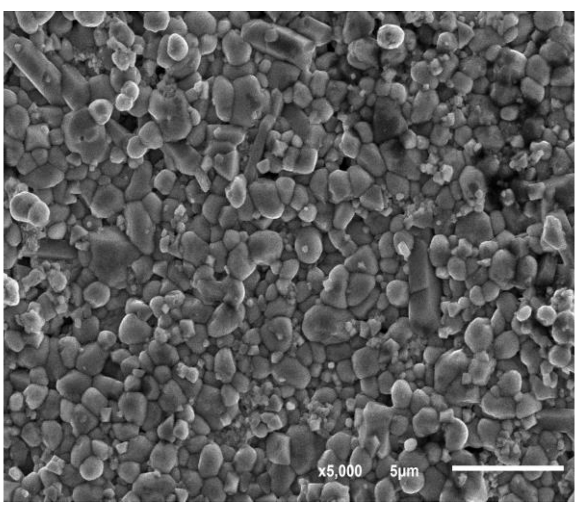

M0-CeO_2-0.5-900

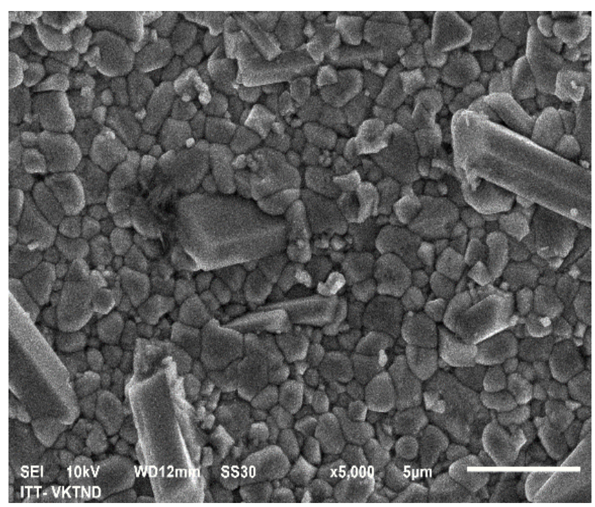

M0-CeO2-0.5-950

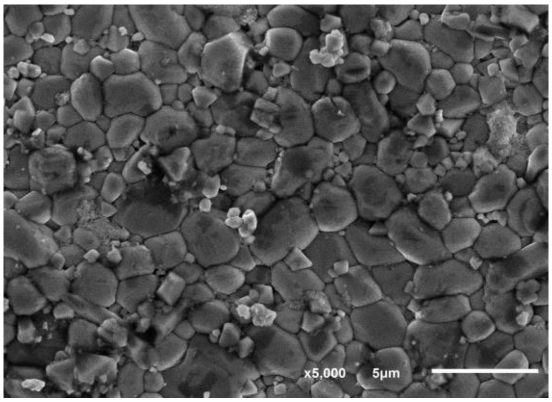

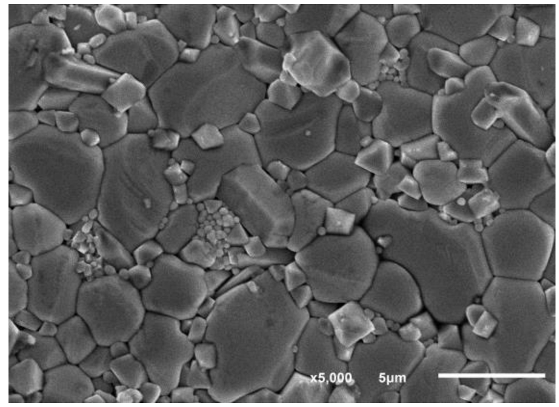

M0-CeO_2-0.5-1000 M0-CeO_2-0.5-1100

Figure 5: *SEM micrographs of the samples with 0.5% content of Y_2O_3/CeO_2 at different sintered temperature (900; 950; 1000; 1100^{0}C)*

The electrical characteristics of the investigated samples are detailed in Figure 6 and Table 2 below. Results demonstrate a consistent trend in the variations of electrical properties for both the undoped sample (M0) and the rare earth-doped sample (M0 with rare earth additives) as the sintering temperature increases. The threshold voltage values of all samples decrease with escalating sintering temperature, while the nonlinear coefficient values exhibit a corresponding reduction. The substantial decrease in threshold voltage values with increasing sintering temperature aligns with the structural analysis discussed earlier. A notable decline in threshold voltage values is observed when the sintering temperature increases from 950 to 1000°C. The highest nonlinear coefficient value achieved is 45 for the sample with 0.5% Y_2O_3 doping at 1100°C. However, it is noteworthy that this sample exhibits a relatively low threshold voltage (only 620 V/mm) compared to other samples. Hence, the choice of sintering conditions should be tailored depending on the specific application requirements. For samples necessitating a high nonlinear coefficient, an increase in sintering temperature is advisable. Furthermore, our observations indicate that the addition of CeO_2 does not yield significant improvements in electrical properties for the investigated system.

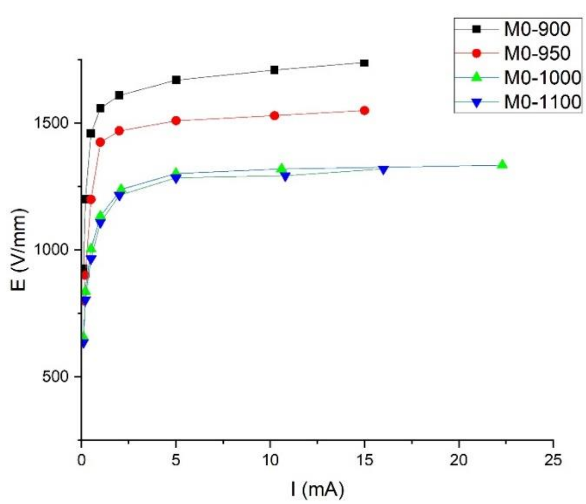

a)

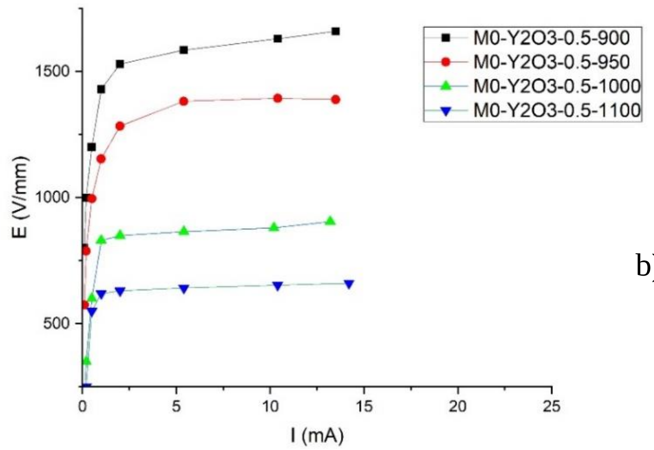

b)

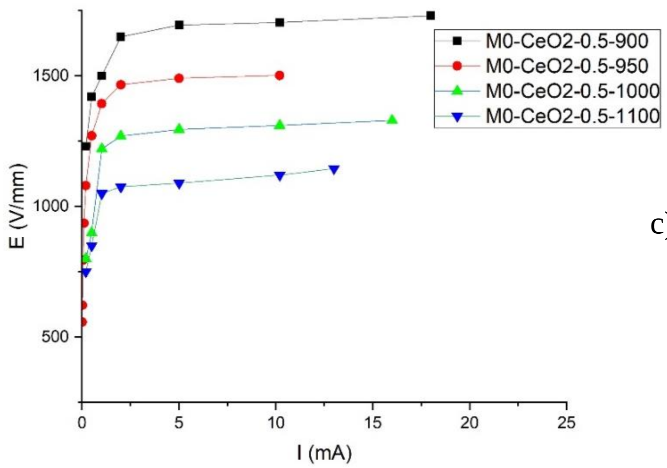

c)

Figure 6: *E-J curves of samples doped with 0.5 % mol of Y_2O_3 (b) and CeO_2 (c) at different sintered temperature in comparison with M0 (a)*

Table 2: *E-J parameters of samples without/with 0.5%mol content of Y_2O_3/CeO_2 at different sintered temperature*

Samples	E_b (V/mm)	α
M0-900	1560	25
M0-950	1425	32
M0-1000	1180	35
M0-1100	950	42
M0-CeO_2-0.5-900	1500	18
M0-CeO_2-0.5-950	1420	20
M0-CeO_2-0.5-1000	1220	31
M0-CeO_2-0.5-1100	1050	36
M0-Y_2O_3-0.5-900	1430	15
M0-Y_2O_3-0.5-950	1154	35

Samples	E_b (V/mm)	α
M0-Y_2O_3-0.5-1000	830	40
M0-Y_2O_3-0.5-1100	620	45

When compared to various alternative varistor materials outlined in Table 3, the varistor ceramics based on ZnO-Bi_2O_3 -Y_2O_3 (presented in this study) exhibit favorable processing temperatures along with outstanding electrical characteristics.

Table 3. *Electrical properties of rare earth doped ZnO based varistor ceramics and some alternative ceramic materials*

Composition	E_b (V/mm)	α
ZnO-Bi_2O_3 -Y_2O_3 (present work)	620	45
ZnO-Bi_2O_3 -Sc_2O_3 [16]	278	54
ZnO-Bi_2O_3 -Er_2O_3 [17]	280	46
ZnO-Bi_2O_3 -Yb_2O_3 [18]	999	22.3

4. Conclusions

In conclusion, the addition of CeO_2 at various concentrations does not contribute to the enhancement of the electrical properties of the samples. CeO_2-doped samples consistently exhibit lower threshold voltage values and nonlinear coefficient values compared to the undoped M0 sample. The incorporation of Y_2O_3 proves beneficial in improving the nonlinear coefficient, albeit at the expense of a reduction in the withstand threshold voltage of the samples. A Y_2O_3 content of 0.5% strikes a balance between these two factors. The sintering temperature significantly influences the characteristics of the samples. Higher sintering temperatures enhance the nonlinear coefficient but concurrently lead to a substantial decrease in the withstand threshold voltage. A sintering temperature of 950°C appears relatively suitable for the investigated system, providing a balanced compromise between the desired electrical properties. ZnO varistors doped with 0.5 mol% Y_2O_3 demonstrated optimal comprehensive electrical properties, featuring a breakdown field of 620 V/mm and a nonlinear coefficient of 45.

Acknowledgements: The research funding from Ministry of Science and Technology of Vietnam (Grant number: ĐTĐLCN.22/23) was acknowledged. The research is partly funded by the basic research fund of the Institute for Tropical Technology, 2023.

REFERENCES

[1] P. Xie, J. Hu, "Influence of Sintering Temperature and ZrO_2 Dopants on the Microstructure and Electrical Properties of Zinc Oxide Varistors," *IEEE Access*, 7, 140126-140133, 2019. DOI: 10.1109/ACCESS.2019.2941965

[2] T. Senda and R. C. Bradt, "Grain Growth of Zinc Oxide During the Sintering of Zinc Oxide - Antimony Oxide Ceramics," *Journal of the American Ceramic Society*, 74(6), 1296-1302, 1991. DOI: 10.1111/j.1151-2916.1991.tb04101.x

[3] S. C. Pillai, J. M. Kelly, D. E. McCormack and R. Ramesh, "High performance ZnO varistors prepared from nanocrystalline precursors for miniaturised electronic devices," *Journal of Chemistry Materials*, 18, 3926-3932, 2008. DOI: 10.1039/b804793f

[4] A. Boumezoued, K. Guergouri, R. Barille, R. Djamil and Z. Mourad, "Synthesis and characterization of ZnO-based nano-powders: study of the effect of sintering temperature on the performance of ZnO-Bi_2O_3 varistors," *Journal of Materials Science: Materials* I_n *Electronics*, 32, 1-15, 2021. DOI: 10.1007/s10854-020-05062-3

[5] T. T. Liu, M. H. Wang, H. P. Zhang and Z. Y. Zhao, "Sol-gel synthesis of doped nanocrystalline ZnO powders using xanthan gum and varistor properties study," *Journal of Materials Science: Materials* I_n *Electronics*, 26(11), 9056-9062, 2015. DOI: 10.1007/s10854-015-3590-2

[6] S. Anas, P. Mukundan, A. M. Sanoj, V. R. Mangalaraja and S. Ananthakumar, "Synthesis of ZnO based nanopowders via a non-hydrolytic sol gel technique and their densification behaviour and varistor properties," In *Processing and Application of Ceramics*, 4, 7-14, 2010. DOI: 10.2298/PAC1001007A

[7] S. Hingorani, V. Pillai, P. Kumar, M. S. Multani and D. O. Shah, Microemulsion mediated synthesis of zinc-oxide nanoparticles for varistor studies," *Materials Research Bulletin*, 28(12), 1303-1310, 1993. DOI: 10.1016/0025-5408(93)90178-G

[8] K. Hembram, T. N. Rao, R. S. Srinivasa and A.R. Kulkarni, "High performance varistors prepared from doped ZnO nanopowders made by pilot-scale flame spray pyrolyzer: Sintering, microstructure and properties," *Journal of the European Ceramic Society*, 35(13), 3535-3544, 2015. DOI: 10.1016/j.jeurceramsoc.2015.05.035

[9] K. Hembram, D. Sivaprahasam and T. N. Rao, "Combustion synthesis of doped nanocrystalline ZnO powders for varistors applications," *Journal of the European Ceramic Society*, 31(10), 1905-1913, 2011. DOI: 10.1016/j.jeurceramsoc.2011.04.005

[10] V.C. Sousa, A.M. Segadães, M.R. Morelli and R.H.G.A. Kimina, "Combustion synthesized ZnO powders for varistor ceramics," *International Journal of Inorganic Materials*, 1(3), 235-241, 1999. DOI: 10.1016/S1466-6049(99)00036-7

[11] Khalaf, A. A., "Elaboration of ZnO based varistors and the effect of the rare-earths on their electrical behaviour," *Energy Procedia*, 19, 116-127, 2012. DOI: 10.1016/j.egypro.2012.05.192

[12] Ke, L., Yuan, Y., Zhao, H., and Ma, X., "Influence of rare-earth doping on the electrical properties of high voltage gradient ZnO varistors," *Ceram-Silikaty*, *57*(1), 53-57, 2013. DOI: 10.1155/2013/726314

[13] He, J., Hu, J., and Lin, Y., "ZnO varistors with high voltage gradient and low leakage current by doping rare-earth oxide," *Science in China Series E: Technological Sciences*, 51(6), 693-701, 2008. DOI: 10.1007/s11431-008-0085-x

[14] Aguilar-Martínez *et al.*, "Effect of sintering temperature on the electric properties and microstructure of SnO2-Co3O4-Sb2O5-Cr2O3 varistor ceramic," *Ceramics International*, *39*(4), 4407-4412, 2013. DOI: 10.1016/j.ceramint.2012.11.030

[15] Cotrim, G. *et al.*, "Tunable capacitor-varistor response of CaCu3Ti4O12/CaTiO3 ceramic composites with SnO2 addition," *Materials Characterization*, *170*, 110699, 2020. DOI: 10.1016/j.matchar.2020.110699

[16] Xu, D., Cheng, X., Zhao, G., Yang, J., and Shi, L., "Microstructure and electrical properties of Sc2O3-doped ZnO-Bi2O3-based varistor ceramics," *Ceramics International*, *37*(3), 701-706, 2011. DOI: 10.1016/j.ceramint.2010.09.032

[17] Zhang, L., Liu, W., Gao, J., Kong, F., Li, Y., and Li, S., "Effects of the Er2O3 doping on the microstructure and electrical properties of ZnO-Bi2O3 based varistor ceramics," *Ceramics International*, *47*(22), 32349-32356, 2021. DOI: 10.1016/j.ceramint.2021.08.132

[18] Xu, D., Tang, D. M., Lin, Y. H., Jiao, L., Zhao, G. P., and Cheng, X. N., "Influence of Yb2O3 doping on microstructural and electrical properties of ZnO-Bi2O3-based varistor ceramics," *Journal of Central South University*, *19*(6), 1497-1502, 2021. DOI: 10.1007/s11771-012-1167-2

TÓM TẮT

ẢNH HƯỞNG CỦA OXIT KIM LOẠI HIẾM ĐẾN CẤU TRÚC VÀ TÍNH CHẤT ĐIỆN CỦA VARISTOR DỰA TRÊN $ZnO-Bi_2O_3$: PHÂN TÍCH, SO SÁNH GIỮA Y_2O_3 VÀ CeO_2

Nguyễn Trung Huy[1], Nguyễn Văn Tráng[1], Cao Thị Hồng[1], Nguyễn Thị Xuyên[1], Võ Thị Kiều Anh[1], Nguyễn Quang Dương[1], Nguyễn Tuấn Anh[1],Lê Đăng Quang[1], Đỗ Quang Thẩm[1]

Viện Kỹ thuật nhiệt đới, Viện Hàn lâm Khoa học và Công nghệ Việt Nam

Ngày nhận bài 27/02/2024, ngày nhận đăng 08/4/2024

Các loại gốm varistor dựa trên oxit kẽm (ZnO), kết hợp với lượng Y_2O_3/CeO_2 khác nhau, được sản xuất thông qua phương pháp phản ứng thể rắn hai bước bao gồm quá trình tiền xử lý và quá trình nung chảy sau đó. Bột ZnO và các chất phụ gia tương ứng được sử dụng làm nguyên liệu trong quá trình sản xuất. Việc nghiên cứu về thành phần pha, cấu trúc vi mô và tính chất điện được thực hiện thông qua các kỹ thuật như nhiễu xạ tia X (XRD), kính hiển vi điện tử quét (SEM) và đo điện trở dòng điện một chiều trực tiếp. Kết quả cho thấy rằng gốm varistor được nung ở 950°C, sử dụng bột được nung qua ở 800°C và pha trộn với lượng Y_2O_3 phù hợp, đã cho thấy tính chất điện được cải thiện. Ngược lại, việc thêm vào nồng độ khác nhau của CeO_2 không góp phần cải thiện các đặc tính điện. Các mẫu được pha trộn với CeO_2 hiển thị điện áp ngưỡng thấp hơn và hệ số phi tuyến chưa được cải thiện so với mẫu không pha trộn (M0). Việc thêm Y_2O_3 đã chứng tỏ hiệu quả trong việc cải thiện hệ số phi tuyến nhưng dẫn đến giảm khả năng chịu điện áp ngưỡng của các mẫu. Hàm lượng Y_2O_3 là 0,5% tương đối phù hợp, cân bằng cả hai yếu tố. Đáng chú ý, varistor ZnO pha trộn với 0,5 mol% Y_2O_3 đã cho thấy tính chất điện tổng hợp tối ưu, với giá trị E_b 620 V/mm và hệ số phi tuyến là 45. Những kết quả cho thấy rằng pha trộn Y_2O_3 hứa hẹn thu được được gốm varistor với hiệu suất điện được tăng cường, đặc biệt là giá trị hệ số phi tuyến.

Từ khoá: Tính chất điện; oxit đất hiếm; $ZnO-Bi_2O_3$ varistor; CeO_2; Y_2O_3.